JOURNAL OF GUIDANCE, CONTROL, AND DYNAMICS
Vol. 25, No. 3, May–June 2002

Semi-Analytical Formulas for Launcher Performance Evaluation

Emanuele Di Sotto* and Paolo Teofilatto†
University of Rome "La Sapienza," 00184 Rome, Italy

A method for the evaluation of launch vehicle performance is presented. The method avoids the CPU-intensive computations needed to find a launch trajectory by a numerical optimization program, and it is based on variation of velocity balance formulas previously introduced. These formulas have been extended to allow a more realistic model of the launcher, including multistaging, variable thrust, nonlinear mass rate, etc. The results obtained show that accuracy is good, because the error in the estimate of the maximum payload mass that can be inserted into required orbits is below 10%. Moreover, the formulas developed can provide, in a very short time, a complete trajectory that can be a suitable input for trajectory optimizers.

I. Introduction

IN the early design phase of the project of a new launcher, it is important to have some fast tool for launcher performance evaluation. Such a tool has to be sufficiently accurate to drive the design choices and must eliminate the lengthy computations needed to find optimal trajectories.

Launcher performance evaluation based on optimal trajectory determination may require many hours of computation on powerful workstations and must be supported by a specialist who has to provide the optimizer with suitable input to allow convergence. Thus, an elementary method of launcher performance evaluation, not requiring any particular skill of the user, is useful. For that reason, a long time ago, a paper-and-pencil launcher performance evaluation was introduced, based on the concept of velocity variation balance:

$$\Delta V = c\log(m_0/m_f) - \Delta V_g - \Delta V_a - \Delta V_c - \Delta V_d$$

where c is the exhaust speed of the rocket propellant and m_0 and m_f are the initial and final mass, respectively. The term $c\log(m_0/m_f)$ is the velocity provided by the launcher propulsion units (Tziolkowski law) and the other ΔV are the so-called gravity, aerodynamic, pressure and disalignment losses.

If the preceding variation of velocity balance is positive, the target orbit may be achieved with final mass m_f. The final mass is the sum of a structural mass m_s and a payload mass m_u : $m_f = m_s + m_u$. The maximum m_u, which still gives positive balance, is an evaluation of the maximum payload mass that can be inserted into the target orbit (launcher performance). The key point is the correct evaluation of such ΔV losses: The known methods of evaluation (for instance, Refs. 1 and 2) are too inaccurate to be useful; errors up to 60% can result from such methods.

In the present paper, a method for ΔV loss and launch performance evaluation is proposed, based on a fast and sufficiently accurate estimate of the launcher trajectory. Results show that a much better accuracy is obtained using this method, the error in the payload mass being below 10%. The target of both a fast and accurate algorithm for launcher performance evaluation seems to be reached and several other results emerge. Some crucial points in launcher trajectory computation have been dealt with. One of these is the choice of the kick angle, which is the angle the thrust vector makes with the vertical direction a few seconds after the launch. Small differences in the kick angle produce very different conditions at the end of the gravity turn trajectory. Despite this sensitivity, the kick angle can be chosen easily in the present approach because the gravity turn trajectory is computed analytically. In fact, a solution proposed by Culler and Fried[3] has been extended here to provide a more realistic model of the launcher including multistaging, variable thrust, and nonlinear mass rate. Moreover, in a very short time, the semi-analytical formulas developed give a complete trajectory that provides suitable input for numerical trajectory optimizers.

The paper is organized as follows. In Sec. II, the formulas for velocity losses are recalled. To have a useful estimate of these velocity losses, it is necessary to determine the trajectory with sufficient accuracy, and Sec. III is devoted to the analytical computation of the gravity turn phase. These gravity turn trajectories are compared to the ones obtained by numerical integration: Comparison shows that the formulas introduced are very accurate. In Sec. IV, the trajectory is completed: A coasting and guided phase lead the launcher to the target altitude. The analysis of Secs. III and IV allows a fast computation of the state trajectory variables. These are used to evaluate ΔV losses and launcher performance. Several examples, reported in Sec. IV, show that the estimated payload mass m_u is fairly close to the one obtained by a numerical program, which solves the launcher trajectory optimization problem in its full generality, with m_u as cost function.

II. Velocity Variation Balance

The launcher velocity variation is governed by the differential equation (the lift force being neglected):

$$\frac{\mathrm{d}V}{\mathrm{d}t} = \frac{T}{m}\cos(\alpha) - g\sin(\gamma) - \frac{D}{m} \tag{1}$$

where α is the angle between the inertial velocity vector $\boldsymbol{V}$ and the longitudinal axis of the launcher; γ is the flight-path angle, that is, the angle between $\boldsymbol{V}$ and the local horizontal direction; T is the thrust; m is the launcher mass; $g = \mu/r^2$ is the gravity; and D is the atmospheric drag (see Ref. 4). Integration of Eq. (1) gives

$$\Delta V = \int_0^{t_f} \frac{T}{m}\,\mathrm{d}\tau - \Delta V_g - \Delta V_a - \Delta V_c - \Delta V_d$$

In the preceding formula, the total velocity variation ΔV is given by the Tziolkowski term minus the gravitational, aerodynamical, overpressure, and disalignment losses. These are defined as follows. The gravity loss is defined by

$$\Delta V_g = \int_0^{t_f} \frac{\mu}{r^2}\sin(\gamma)\,\mathrm{d}t = g\int_0^{t_f}\sin(\gamma)\,\mathrm{d}t \tag{2}$$

where a constant gravitational field is assumed. The aerodynamic loss is defined by

$$\Delta V_a = \int_0^{t_f} \frac{D}{m}\,\mathrm{d}t \tag{3}$$

Received 31 May 2001; revision received 30 October 2001; accepted for publication 2 November 2001.

*Doctorate Student, Scuola di Ingegneria Aerospaziale, v. Eudossiana 18; currently Project Engineer, Grupo de Mechanica del Vuelo Madrid, Calle Isaac Newton 11, P.T.M.-Tres Cantos E-28760 Madrid, Spain.

†Associate Professor, Aerospace Department, v. Eudossiana 18.

The overpressure loss is defined by

$$\Delta V_c = \int_0^{t_f} (\text{press} \times S_u)\, dt \tag{4}$$

where press is the external pressure at the current altitude and S_u is the engine nozzle surface. This term ΔV_c maximizes the possible thrust loss (hence, the related velocity loss) due to possible flow overexpansion that may occur for lauchers equipped with constant geometry nozzles. The disalignment loss is defined by

$$\Delta V_d = \int_0^{t_f} \frac{T}{m}[1 - \cos(\alpha)]\, dt \tag{5}$$

and measures how much variation of velocity is lost when the thrust direction is not parallel to the direction of the velocity ($\alpha \neq 0$).

These ΔV losses depend on the launcher state variables, that is, on the launcher trajectory. An estimate of the ΔV losses is useful: the given balance between the velocity variation provided by the engines (Tziolkowski term) and the velocity losses would make clear if the target orbit can be reached for a given mass budjet and would provide an evaluation of the launcher performance. To get a good estimate of ΔV losses, the launch vehicle trajectory will be defined starting from the gravity turn phase.

III. Gravity Turn Phase

The aerodynamic loads acting on the launcher during the atmospheric part of the trajectory constrain the steering law to keep the angle α close to zero. In this phase, the gravity field turns the velocity vector direction from the local vertical, and so this arc of the launcher trajectory is called gravity turn. The gravity turn is quite sensible on the initial angle between the velocity vector and the local vertical direction, the so-called kick angle χ_0. This angle is achieved a few seconds after the liftoff by a rotation of the launcher about its transversal axis (pitchover maneuver).

Figure 1 shows the values of the perigee altitudes reached at the third-stage burnout of a four-stage launcher with parameters defined in the Appendix. All of the three stages of the launcher followed a gravity turn trajectory starting from different values of the kick angle χ_0 chosen in the interval [4.9, 6.2 deg]. Fixing the kick angle χ_0, the position and velocity reached by the third stage are computed: these give the semi-axis and the eccentricity, hence the perigee height, of the orbit that the launcher would follow in a coasting phase. The five values marked by a circle in Fig. 1 generate orbital conditions (perigee greater than Earth radius), the other values, marked by a plus sign, have perigee lower than the Earth radius. Note that the orbital conditions are achieved only for χ_0 in the small range $\Delta = [5.31, 5.34 \text{ deg}]$. For any other choice of the kick angle, the launcher falls to Earth (see Ref. 5). The kick angles in the interval Δ correspond

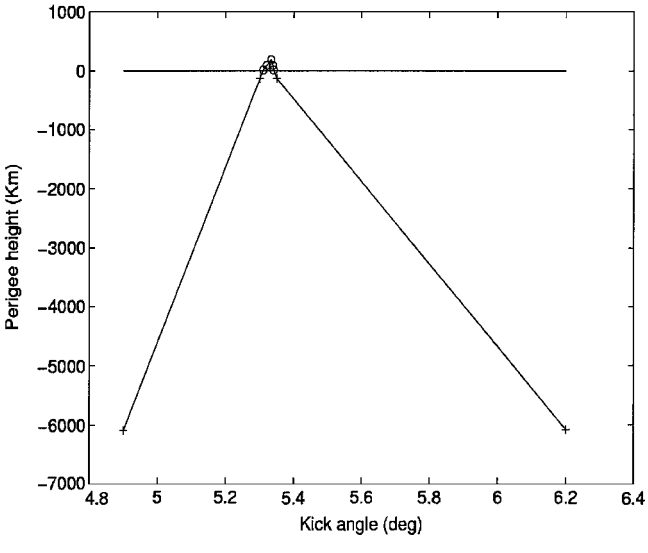

Fig. 1 Perigee altitude reached by the first three stages in gravity turn trajectory vs kick angle.

Table 1 Perigee altitudes reached by gravity turn trajectories at third-stage burnout

Kick angle, deg	γ_f, deg	Perigee altitude, km
6.200	−5.00	−6078
5.350	−0.10	−135
5.340	−0.07	11
5.388	−0.05	90
5.333	0.00	184
5.320	0.05	91
5.310	0.07	11
5.300	0.10	−135
4.900	5.00	−6091

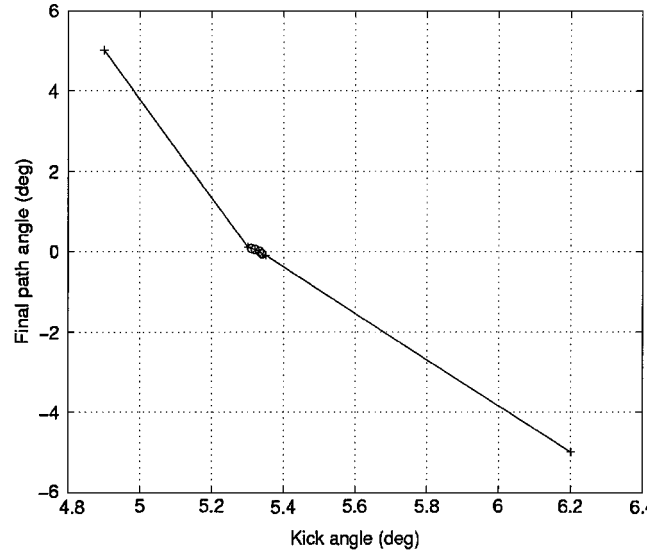

Fig. 2 Final flight-path angle reached by the first three stages in gravity turn trajectory vs kick angle; trajectories reaching orbital conditions have final flight-path angle close to zero.

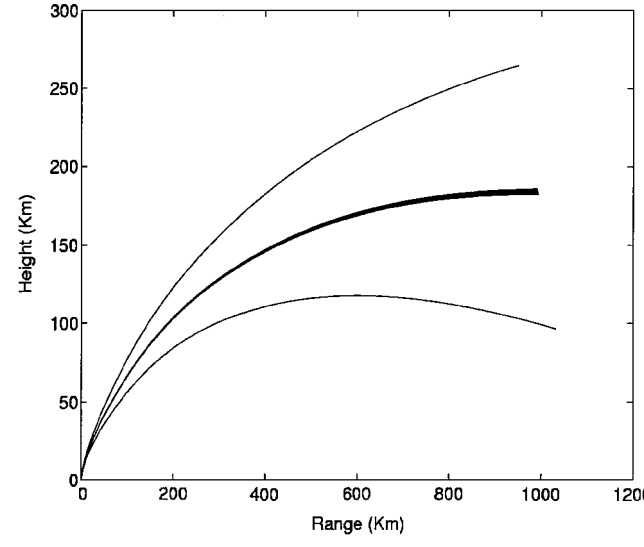

Fig. 3 Gravity turn trajectories performed by the first three stages for different values of kick angle; trajectories reaching orbital conditions are in the middle.

to those trajectories having an almost vanishing flight-path angle γ_f at the end of the gravity turn (Fig. 2 and Table 1). Note that the maximum perigee altitude is reached by the trajectory with $\gamma_f = 0$, that is, the flattest trajectory (Fig. 3). In fact the gravity loss formula (2) of Sec. II states that ΔV_g depends on $\sin(\gamma)$, that is, gravity loss is bigger for steep ascent trajectories with respect to flat ones. Then, in the definition of the launch trajectory, it is reasonable to select the kick angle χ_0 that would generate a gravity turn with $\gamma_f = 0$

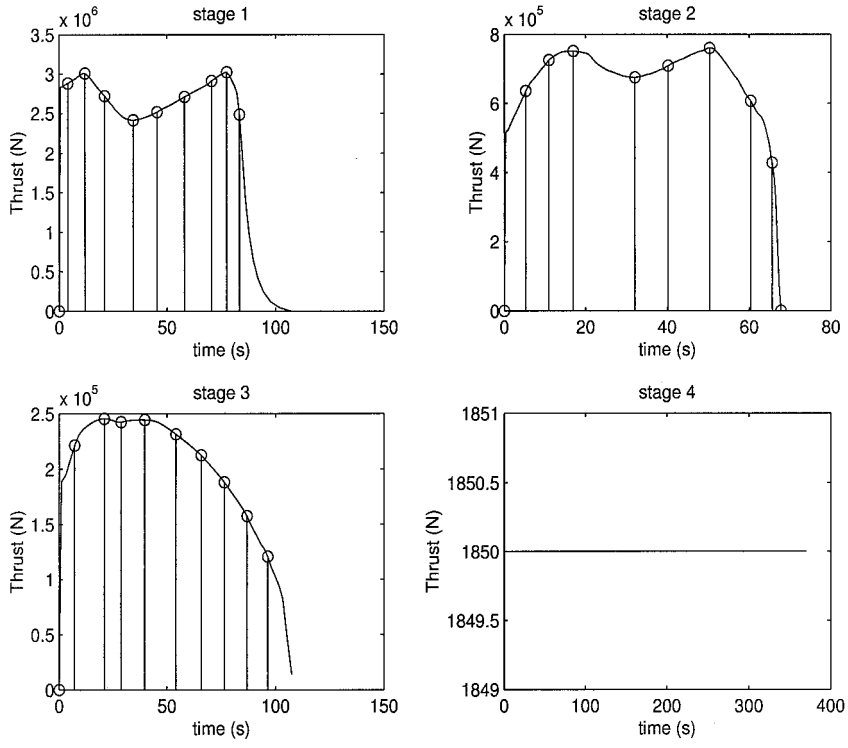

Fig. 4 Thrust (in newton) variations of a four-stage launcher.

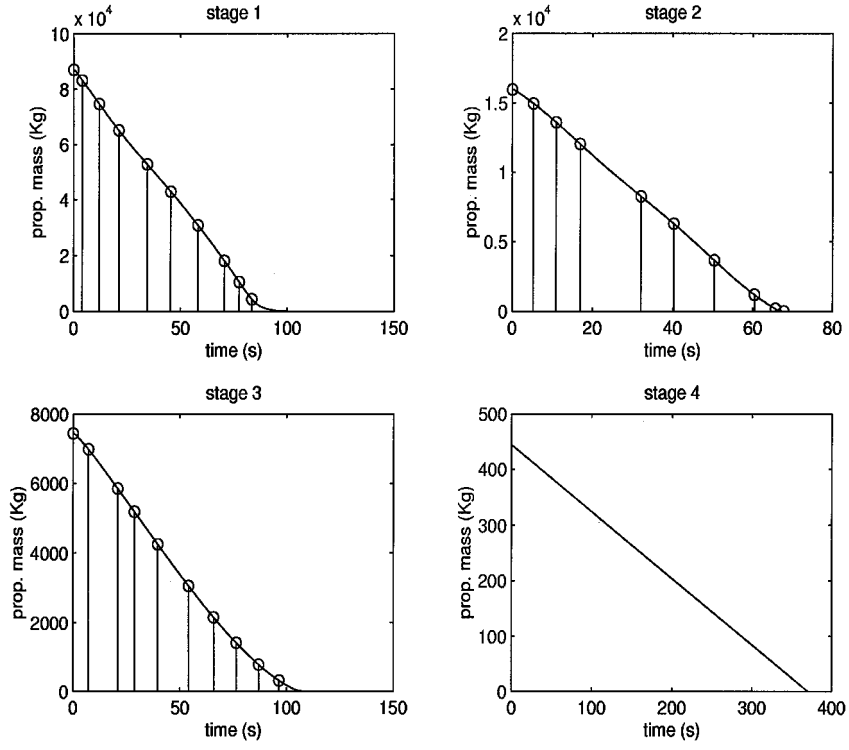

Fig. 5 Propellant mass (in kilogram) variation of a four-stage launcher.

at the third-stage burnout. The search for χ_0 leads to a two-point boundary-value problem whose input are generally tabulated data of thrust, mass, and mass rate as a function of time. Figure 4 shows the thrust, and Fig. 5 shows the propellant mass variations with time for the four-stage launcher reported in the Appendix. To solve such a two-point boundary-value problem in short time, it is convenient to rely on a simplified model allowing semi-analytic solutions, and the accuracy of these solutions will be improved relaxing some of the assumptions introduced in the simplified model.

Exact solutions of the gravity turn trajectory are known under the following two conditions on thrust and mass variations: Condition A is constant thrust to weight ratio[3,4,6] and condition B is constant thrust and linear propellant mass variation.[3] In addition, the following assumptions are made: 1) single-stage launcher, 2) aerodynamic forces neglected, 3) nonrotating Earth, 4) planar launch, and uniform gravitational field.

For completeness, the derivation of the solutions proposed in Ref. 3 under conditions A or B and assumptions 1–5 will be

presented. Then more general formulas will be introduced to remove restrictions 1–4.

Under assumptions 1–5 the gravity turn equations are

$$\dot{V} = T/m - g\sin(\gamma), \qquad V\dot{\gamma} = -g\cos(\gamma) \tag{6}$$

or, as a function of the pitch angle $\chi = \pi/2 - \gamma$,

$$\dot{V} = T/m - g\cos(\chi), \qquad \dot{\chi} = g/V\sin(\chi) \tag{7}$$

The transformation

$$z = \tan(\chi/2)$$

allows to express the trigonometrical functions of Eq. (7) as ratios of polynomials:

$$\cos(\chi) = \frac{1-\tan^2(\chi/2)}{1+\tan^2(\chi/2)} = \frac{1-z^2}{1+z^2}$$

$$\sin(\chi) = \frac{\tan(\chi/2)}{1+\tan^2(\chi/2)} = \frac{2z}{1+z^2}$$

Moreover,

$$\dot{z} = \frac{\dot{\chi}/2}{\cos^2(\chi/2)}$$

then

$$\dot{\chi} = 2\dot{z}/(1+z^2) = (g/V)[2z/(1+z^2)]$$

where the last equality follows from the second equation in Eq. (7). Then Eqs. (7) become

$$\dot{V} = T/m - g[(1-z^2)/(1+z^2)], \qquad \dot{z} = (g/V)z \tag{8}$$

The ratio of the two equations gives the single equation

$$\frac{\mathrm{d}V}{\mathrm{d}z} = \left(\frac{n}{z} - \frac{1-z^2}{1+z^2}\frac{1}{z}\right)V, \qquad n = \frac{T}{mg} \tag{9}$$

If condition A holds true, n is constant and the variables in Eq. (9) can be separated, thus leading to the known solution:

$$V = Az^{n-1}(1+z^2) \tag{10}$$

$$t = (A/g)z^{n-1}[1/(n-1) + z^2/(n+1)] \tag{11}$$

In Eq. (10), A is determined by the initial conditions V_0 and z_0. In fact, under the preceding assumptions, the initial launching conditions (that is, launcher on the vertical and staying on the launch pad) correspond to the values $V_0 = 0$ and $\chi_0 = z_0 = 0$. As observed in Ref. 3, formulas (10) and (11) satisfy the differential equation with the given initial conditions irrespective of the value of A. This is because of the singularity of Eq. (8) for $V = 0$, so that the Cauchy problem with the initial launching conditions does not select a unique solution, but rather a one-parameter family of solutions with parameter A. This fact is not merely a mathematical curiosity; actually the parameter A is used here to select the solution of the family having the desired final conditions. In the present case, this means imposing that the solution has a vanishing flight-path angle at launcher burn time t_b, that is, $z_f = 1$ when $t = t_b$. From formula (11), one obtains

$$A = (g/2)[(n^2-1)/n]t_b \tag{12}$$

Formula (10) with A taken from Eq. (12) gives the gravity turn velocity corresponding to initial launching conditions $V_0 = 0$ and $\chi_0 = 0$ and final condition $\gamma_f = 0$.

To supress assumption 1, solution (10–12) is now generalized to multistage launchers. Let the case of a three-stage launcher be considered, with constant thrust to weight ratios n_1, n_2, and n_3. For each of the three stages, there are equations such as Eqs. (9) and (10) with variables (V_i, z_i), $i = 1, 2, 3$. Then the following formulas are obtained by separation of variables:

$$V_1 = A_1 z_1^{n_1-1}\left(1+z_1^2\right), \qquad t_{b1} = \frac{A_1}{g}z_{1f}^{n_1-1}\left(\frac{1}{n_1-1} + \frac{z_{1f}^2}{n_1+1}\right) \tag{13}$$

$$V_2 = A_2 z_2^{n_2-1}\left(1+z_2^2\right)$$

$$t_{b2}^* - t_{b1} = \frac{A_2}{g}\left[z_{2f}^{n_2-1}\left(\frac{1}{n_2-1} + \frac{z_{2f}^2}{n_2+1}\right) - z_{20}^{n_2-1}\left(\frac{1}{n_2-1} + \frac{z_{20}^2}{n_2+1}\right)\right] \tag{14}$$

$$V_3 = A_3 z_3^{n_3-1}\left(1+z_3^2\right)$$

$$t_{b3}^* - t_{b2}^* = \frac{A_3}{g}\left[z_{3f}^{n_3-1}\left(\frac{1}{n_3-1} + \frac{z_{3f}^2}{n_3+1}\right) - z_{30}^{n_3-1}\left(\frac{1}{n_3-1} + \frac{z_{30}^2}{n_3+1}\right)\right] \tag{15}$$

where t_{b2}^* is the sum of the burn times of the first two stages: $t_{b2}^* = t_{b2} + t_{b1}$, and t_{b3}^* is the sum of the three burn times: $t_{b3}^* = t_{b3} + t_{b2} + t_{b1}$. In formulas (13–15) A_i, z_{if}, and z_{i0} are unknown constants, which will be determined as follows. The required final condition is $z_{3f} = 1$, and for continuity of the solution one must have

$$z_{1f} = z_{20}, \qquad z_{2f} = z_{30} \tag{16}$$

$$V_{1f} = V_{20}, \qquad V_{2f} = V_{30} \tag{17}$$

This means that the state variables at a stage burnout must be equal to state variables at the ignition of the following stage (at this point, no coasting phase is considered). The first equality in Eq. (17) reads

$$V_{1f} = A_1 z_{1f}^{n_1-1}\left(1+z_{1f}^2\right) = V_{20} = A_2 z_{20}^{n_2-1}\left(1+z_{20}^2\right)$$

Because of Eq. (16), one has

$$A_1/A_2 = z_{20}^{n_2-n_1} \tag{18}$$

and in the same way, one gets

$$A_2/A_3 = z_{30}^{n_3-n_2} \tag{19}$$

Equations (18) and (19) together with the following three equations [taken from formulas (13–15) and constraints (16)]

$$t_{b1} = \frac{A_1}{g}z_{20}^{n_1-1}\left(\frac{1}{n_1-1} + \frac{z_{20}^2}{n_1+1}\right)$$

$$t_{b2} = \frac{A_2}{g}\left[z_{30}^{n_2-1}\left(\frac{1}{n_2-1} + \frac{z_{30}^2}{n_2+1}\right) - z_{20}^{n_2-1}\left(\frac{1}{n_2-1} + \frac{z_{20}^2}{n_2+1}\right)\right]$$

$$t_{b3} = \frac{A_3}{g}\left[2\frac{n_3}{n_3^2-1} - z_{30}^{n_3-1}\left(\frac{1}{n_3-1} + \frac{z_{30}^2}{n_3+1}\right)\right]$$

give five equations in the five unknowns A_1, A_2, A_3, z_{20}, and z_{30}. It is possible to solve for the unknown values, then get the solution (13–15) of the three-stage gravity turn trajectory with final condition $\gamma_f = 0$.

In the preceding formulas, condition A forces consideration of average thrust and mass values $\overline{Tr}_i$ and $\bar{m}_i$ for each of the three stages and definition of $n_i = \overline{Tr}_i/\bar{m}_i$. A more realistic result can be obtained considering each stage i composed by $N_i - 1$ virtual substages, if N_i is the number of tabulated thrust and mass data available for stage i. For instance, in the example of Fig. 4, stage 1 is composed of 10 virtual substages, stage 2 of 9 virtual substages, and stage 3 of 10 virtual substages. The preceding formulas can be applied considering constant thrust to weight ratios n_{ij} for each

substage and imposing boundary conditions analogous to Eqs. (16) and (17) between each pair of consecutive virtual substages.

Moreover, a more accurate trajectory can be obtained applying the same procedure with the condition B of linear mass decrement in each of the substages, thus generalizing to multistage launchers the gravity turn solution of Ref. 3.

To obtain their gravity turn solution under condition B, Culler and Fried[3] introduced the transformation

$$z = e^{\phi}$$

which makes system (8) equal to

$$\frac{\mathrm{d}V}{\mathrm{d}t} = \frac{T}{m} + g\, tgh(\phi), \qquad V\frac{\mathrm{d}\phi}{\mathrm{d}t} = g \tag{20}$$

Integration of the first equation gives

$$V(t) = \int_0^t \frac{T}{m}\,\mathrm{d}t + g\int_0^t tgh[\phi(\tau)]\,\mathrm{d}\tau \tag{21}$$

where the first integral is the Tziolkowski term and the second one is the gravity loss. Integrating the second of Eqs. (20), one obtains

$$\phi(t) = -\int_t^{t_f} \frac{g}{V}\,\mathrm{d}\tau + \phi(t_f)$$

that is,

$$\phi(t) = -\int_t^{t_f} \left\{ g \Big/ \left[\int_0^{\tau} \frac{T}{m}\,\mathrm{d}s + g\int_0^{\tau} tgh(\phi)\,\mathrm{d}s \right] \right\} \mathrm{d}\tau - k \tag{22}$$

where k is related to the (required) final flight-path angle:

$$k = -\phi(t_f) = -\log[z(t_f)] = -\log[\tan(\chi_f/2)]$$
$$= -\log(\tan\{[(\pi/2) - \gamma_f]/2\}) \tag{23}$$

Because the initial condition $z_0 = 0$ would imply

$$\lim_{t\to 0} \phi(t) = -\infty$$

the further transformation has been defined in Ref. 3:

$$\psi = tgh(\phi)$$

The variable ψ has the correct boundary condition,

$$\psi(0) = -1 \tag{24}$$

and it satisfies the integral equation,

$$\psi(t) = tgh\left\{ \int_t^{t_f} \left[g \Big/ \left(\int_0^{\tau} \frac{T}{m}\,\mathrm{d}s + g\int_0^{\tau} \psi\,\mathrm{d}s \right) \right] \mathrm{d}\tau - k \right\} \tag{25}$$

The solution of the integral equation (25) is found by iterations, starting with the initial choice $\psi(t) = -1$ for any t, which clearly satisfies the boundary condition (24). To generalize the Culler–Fried solution (25) to multistage launchers, allowing also virtual substages, the following formula is here introduced:

$$\psi(t) = tgh\left\{ \int_t^{t_f} \left[g \Big/ \left(\int_0^{\tau} \sum_{ij} \frac{T_{ij}}{m_{ij}}\delta_{ij}\,\mathrm{d}s + g\int_0^{\tau} \psi\,\mathrm{d}s \right) \right] \mathrm{d}\tau - k \right\} \tag{26}$$

In formula (26), $\delta_{ij}(t) = 1$ if t is lower than the (total) burning time of the stage i ($t < t^*_{b_i}$) and within the interval of the virtual substage j; in all other cases, $\delta_{ij}(t) = 0$. Once ψ has been found, formula (21) allows the computation of both the gravity loss and the velocity profile of the gravity turn trajectory having the assigned final path angle. In formula (26), k is the parameter of the family of gravity turn trajectories having initial launching conditions $V(0) = 0$ and $\chi(0) = 0$ (as A was the parameter for the same solutions under condition A) and it can be related to the final flight-path angle γ_f. For instance, the gravity turn with a zero final path angle γ_f corresponds to $z(t_f) = 1$; hence, $k = 0$ [see formula (23)].

Table 2 Trajectory data errors at second-stage separation

Parameter	Value
V_f, m/s	1.8
γ_f, deg	2.6
Altitude, km	1.1

The results given by formulas (21) and (26) have been compared to the results obtained by a numerical program that solves the trajectory optimization problem defined in full generality and having the maximum payload mass as a cost function.

In the following test, the numerical program has been run under assumptions 1 and 2 (no drag and no Earth rotation), the target orbit is circular of altitude of 1200 km and inclination $i = 100$ deg. The numerical program finds the optimal kick angle, the optimal coasting time, and some guidance parameters for the third-stage trajectory to have maximum payload at the target orbit. Table 2 shows the errors of the preceding gravity turn formulas with respect to the results of the numerical optimization program at the time of the second-stage burn out (the same payload mass m_u is assumed in the two algorithms). It is apparent that the preceding formulas give a quite an accurate result for the velocity and height values, whereas an error occurs in the flight-path angle. This error is related to the flat Earth approximation in formulas (21) and (26). In fact, if the Earth curvature is taken into account by the formula

$$\delta\gamma = \tan^{-1}(X/R_E)$$

where X is the range value and R_E the Earth radius, the correction to the γ value

$$\gamma \longrightarrow \gamma + \delta\gamma$$

makes the error in γ lower than 0.2 deg.

It turns out that the gravity turn phase, neglecting drag and Earth rotation, is very well modeled by formulas (21) and (26), and the choice $\gamma_f = 0$ in the formulas makes the result close to the optimal one. Moreover, the problem of the choice of the kick angle has been circumvented: In the preceding semi-analytical gravity turn trajectories, the kick angle is an output of the a priori choice to have flight-path angle equal to zero at the end of the third-stage gravity turn trajectory, that is, $\gamma_f = 0$ for $t = t^*_{b_3}$.

In fact, the gravity turn trajectory will be followed only in the atmospheric flight, typically till the second-stage burnout. At that time, to include drag and Earth rotation effects, the velocity will be updated as described in the next section.

IV. ∇V Loss Evaluation and Guided Phase

At the end of atmospheric flight, the velocity V_G and flight-path angle γ are corrected to make the assumptions 2–4 of the preceding section less restrictive. The aerodynamic drag effect can be taken into account by evaluating, using formula (3), the ΔV_a aerodynamic loss along the gravity turn trajectory $V_G(t)$, $\gamma(t)$ obtained in the preceding section. The overpressure loss ΔV_c can be computed by formula (4). Then restriction 2 is relaxed by subtracting $\Delta V_a + \Delta V_c$ from the gravity turn velocity V_G at the end of the atmospheric flight.

To remove assumptions 3 and 4, the following arguments are introduced. First the azimuth angle at launch ψ is chosen according to the well-known formula

$$\sin(\psi) = \cos(i)/\cos(\mu)$$

where i is the inclination of the target orbit and μ is the launch site latitude. This choice of the azimuth angle selects the plane Π of the trajectory (provided $i \geq \mu$) (Ref. 7). However, the earlier computation is based on the relative velocity $\boldsymbol{V}_G$ and does not take into account that the launcher has an initial velocity equal to the Earth velocity $\boldsymbol{V}_E = \boldsymbol{\Omega} \wedge \boldsymbol{R}_E$. This velocity has a component in-plane Π, $\boldsymbol{V}_\pi$, and an out-of-plane component $\boldsymbol{V}_n$ (Fig. 6). In Fig. 6

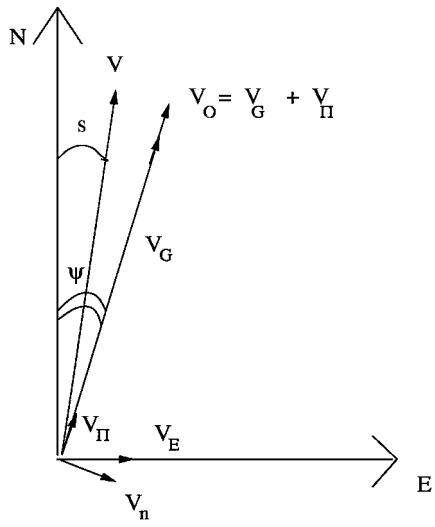

Fig. 6 Determination of the azimuth launch angle.

and in the following formula (29), $\boldsymbol{V}_G$ and $\boldsymbol{V}_\pi$ are regarded as parallel, thus approximating $\cos\gamma_f \sim 1$ and $\sin\gamma_f \sim 0$, with error of order γ_f^2.

The launcher will have the velocity in plane Π:

$$\boldsymbol{V}_0 = \boldsymbol{V}_G + \boldsymbol{V}_\Pi$$

if a different azimuth angle is chosen and a variation of velocity is considered to compensate the out-of-plane velocity $\boldsymbol{V}_n$ (Ref. 8). In fact, let $\boldsymbol{V}$ be the velocity such that

$$\boldsymbol{V} + \boldsymbol{V}_n = \boldsymbol{V}_0 \tag{27}$$

and let s be its azimuth angle (Fig. 6). Relationship (27) gives

$$\boldsymbol{V} = \boldsymbol{V}_0 - \boldsymbol{V}_n \tag{28}$$

and

$$V^2 = \boldsymbol{V} \times \boldsymbol{V} = (\boldsymbol{V}_0 - \boldsymbol{V}_n) \times (\boldsymbol{V}_0 - \boldsymbol{V}_n) = V_0^2 + V_n^2$$

where the last equality holds because $\boldsymbol{V}_0$ and $\boldsymbol{V}_n$ are orthogonal vectors.

The azimuth angle s of $\boldsymbol{V}$ can be found writing Eq. (28) in the north and east components.

North component:

$$V\cos(s) = V_0\cos(\psi) - V_n\sin(\psi)$$

East component:

$$V\sin(s) = V_0\sin(\psi) + V_n\cos(\psi)$$

and dividing the east by the north component,

$$\tan(s) = \frac{V_0\sin(\psi) + V_n\cos(\psi)}{V_0\cos(\psi) - V_n\sin(\psi)}$$

Therefore, to have the velocity $\boldsymbol{V}_0$ in the plane Π, one should have the azimuth angle s and the velocity $\boldsymbol{V}$. Because the velocity provided by the vehicle plus $\boldsymbol{V}_\Pi$ has modulus $V_0 < V$, an extra velocity ΔV_{an} would be necessary in the same direction of $\boldsymbol{V}$ with modulus,

$$\Delta V_{an} = V - V_0 = \sqrt{V_0^2 + V_n^2} - V_0$$

and the correction ΔV_{an} relaxes the assumptions 3 and 4. Note that, as for the other velocity losses, the Earth rotation is entirely compensated at the end of the gravity turn. This choice, although not optimal, allows the consideration of a simple planar guidance law in the exoatmospheric portion of the trajectory.

In summary, the velocity, the flight path, and the azimuth angles are updated at the end of the gravity turn trajectory as follows:

$$V_G \longrightarrow V_G - \Delta V_a - \Delta V_c - \Delta V_{an} + V_\pi$$
$$\gamma \longrightarrow \gamma + \delta\gamma, \qquad \psi \longrightarrow s \tag{29}$$

where the $\delta\gamma$ variation is the one defined in Sec. III.

As mentioned before, it is supposed that the gravity turn ends at second-stage burnout, whereas the third stage, being in a vacuum flight, will follow the optimal steering law hereafter specified. Because γ was imposed to be zero at the end of the three-stage gravity turn, at the second-stage burnout the flight-path angle γ has still a certain value, and it is convenient to allow a coasting phase to reduce γ and increase the height at the price of some velocity loss. Note that the coasting phase can also be included in formulas (21) and (26) considering virtual substages with zero thrust. In such a case, the coasting time becomes an explicit parameter and has to be specified in advance. In the present algorithm the coasting time is determined as the time needed to reduce the flight-path angle to a given value $\gamma_{\min}$, and the optimal value $\gamma_{\min}$ for maximum payload can be found by a parametric search.

After the coasting phase, the third stage is guided according to the linear tangent law:

$$\varphi(t) = \tan^{-1}[\tan(\varphi_0)(1 - t/t_f)] \tag{30}$$

where the pitch angle φ is the angle between the thrust and the horizontal direction. This law maximizes the horizontal velocity u_f, satisfying the final conditions $h(t_f) = h_f$ and $v(t_f) = 0$ (perigee conditions), where h_f is the required orbit height and v is the vertical velocity.[4] The steering law (29) depends on two unknown parameters: the initial value of the steering angle φ_0 and the final time t_f (subject to $t_f \geq t_{b3}$). These unknown parameters are found applying a Newton–Raphson routine to the error vector function: $\boldsymbol{E} = [h(t_f) - h_f, v(t_f)]$. To speed up the computations, the entries of the matrix $(\nabla\boldsymbol{E})^{-1}$ needed in the Newton–Raphson algorithm are evaluated using the semi-analytical formulas of Ref. 9.

The guided phase ends at third-stage burnout, and the disalignment loss can be computed defining the angle of attack $\alpha = \varphi - \gamma$ along the guided trajectory [see formula (5)]. At that time, two variations of velocity are computed: 1) ΔV_1, needed to reach the circular velocity at the current height, and 2) ΔV_2, to move from the previous circular orbit to the target one via a Hohmann-like transfer. These velocity variations should be performed by the fourth-stage engine. The propellant m_n needed to get such two impulsive thrusts is computed and compared to the available propellant m_d. If $m_d - m_n$ is positive, the target orbit can be reached, and some extra weight can be added to the payload mass m_u; otherwise, one must run the algorithm again with a smaller payload mass. In a few iterations, the algorithm finds the payload mass that makes the balance $m_d - m_n$ equal to zero (within a given tolerance), thus providing the user with the following outputs: 1) estimated payload mass, 2) gravity, aerodynamical, overpressure, and disalinement losses 3) coasting time, and 4) azimuth angle.

The estimated payload mass is the maximum payload mass according to the present algorithm for the following reasons:

1) The key parameter γ_f of the gravity turn phase of the trajectory (first and second stages) has been chosen to reduce the gravity loss.

2) The time of the coasting phase has been optimized by a parametric search.

3) The third-stage steering law has been chosen to maximize the perigee velocity at third-stage burnout, thus minimizing the ΔV that has to be provided by the four-stage propellant, in favor of an increased payload mass.

This strategy is compared to the results obtained by a rather accurate trajectory optimization program (the correct values). The trajectory optimizer is based on a hybrid direct/indirect method and finds the following optimal parameters to maximize the payload mass in the required orbit: the azimuth angle, the time and angular velocity of the pitchover maneuver (these determine the kick angle), the coasting time, and three guidance parameters for the third-stage

Table 3 Trajectory data[a] for target orbit h = 700 km, i = 90 deg

Event	t, s	ΔV_c	ΔV_a	ΔV_g	ΔV_d	V_G	V_a	V_N	γ	γ_N	h_a	h_N
Stage 1	101.5	−112	−121	−649	0	2394	2161	2137	21.9	21.2	48	46
Stage 2	169.3	−113	−122	−825	0	4522	4287	4250	10.1	11.0	100	98
Coast	169.3	−113	−122	−825	0	4264	4264	4250	10.1	11.0	100	98
End coast	211.6	−113	−122	−884	0	4207	4207	4176	6.6	6.3	142	131
Stage 3	319.0	−113	−122	−916	−132	7628	7628	7777	0.3	0.1	164	152

[a]All ΔV and velocities V, V_a, and V_n are in meters per second. Angles γ and γ_N are in degrees and h_a and h_N are in kilometers. Estimated payload mass is 1340 kg, payload mass error is 2.0%.

Table 4 Trajectory data[a] for target orbit h = 1200 km, i = 100 deg

Event	t, s	ΔV_c	ΔV_a	ΔV_g	ΔV_d	V_G	V_a	V_N	γ	γ_N	h_a	h_N
Stage 1	101.5	−112	−122	−647	0	2410	2176	2067	21.9	22.0	47	46
Stage 2	169.3	−113	−123	−821	0	4558	4322	4188	10.0	11.1	100	98
Coast	169.3	−113	−123	−821	0	4216	4216	4188	10.0	11.1	100	98
End coast	221.5	−113	−123	−889	0	4151	4151	4106	5.3	5.5	140	134
Stage 3	328.9	−113	−123	−917	−130	7718	7718	7828	0.8	0.1	160	151

[a]All ΔV and velocities V, V_a, and V_n are in meters per second. Angles γ and γ_N are in degrees and h_a and h_N are in kilometers. Estimated payload mass is 1140 kg, payload mass error is 3.6%.

Table 5 Trajectory data[a] for target orbit h = 1500 km, i = 5.2 deg

Event	t, s	ΔV_c	ΔV_a	ΔV_g	ΔV_d	V_G	V_a	V_N	γ	γ_N	h_a	h_N
Stage 1	101.5	−112	−122	−649	0	2396	2162	2539	21.9	17.4	48	46
Stage 2	169.3	−113	−122	−825	0	4527	4292	4663	10.1	10.0	100	98
Coast	169.3	−113	−122	−825	0	4754	4754	4663	10.1	10.0	100	98
End coast	213.3	−113	−122	−889	0	4690	4690	4607	7.0	7.8	130	125
Stage 3	320.7	−113	−122	−931	−127	8213	8213	8086	0.8	0.4	155	154

[a]All ΔV and velocities V, V_a, and V_n are in meters per second. Angles γ and γ_N are in degrees and h_a and h_N are in kilometers. Estimated payload mass is 1390 kg, payload mass error is 6.1%.

trajectory. Tables 3–5 compare the results concerning the following circular target orbits reached from the Kourou launch site:

Table 3, orbit altitude $h = 700$ km and inclination $i = 90$ deg; Table 4, orbit altitude $h = 1200$ km and inclination $i = 100$ deg; and Table 5, orbit altitude $h = 1500$ km and inclination $i = 5.2$ deg. V_a in the footnotes of Tables 3–5 is the velocity minus the drag and overpressure losses, h_a is the altitude obtained integrating the equation $\dot{h} = v \sin(\gamma)$ with the velocity $v = V_a$. Subscript N refers to the results obtained by the numerical optimizator, the correct values. From the second-stage burnout to the beginning of the coasting arch, only the velocity value is updated by the sum of the ΔV_{an} and V_π terms. Tables 3–5 report the values of the payload mass, as well as the relative error of the payload mass evaluation. Note that the errors are well within 10% of relative error.

The method proposed has been applied to a four-stage launcher only for convenience in explaining the method, but it is applicable to any number of virtual or physical stages. For instance, the $\gamma_f = 0$ condition for the selection of the gravity turn trajectory can be imposed to the last stage of a three- or two-stage launcher, or as final condition for a reusable launch vehicle. The stop condition for the gravity turn phase can be changed into the maximum aerodynamic load condition $q\alpha \leq (q\alpha)_{\max}$, where $q = \frac{1}{2}\rho V^2$ is the dynamic pressure and the maximum value of the aerodynamical load $(q\alpha)_{\max}$ is a parameter related to the launcher structure. This condition will be satisfied as soon as the altitude makes the air density ρ small enough. Then, as before, a coasting time can be found by a parametric search and the linear tangent law can be applied to reach the target orbit.

As a further example, the method has been applied to the three-stage launch vehicle with parameters reported in the Appendix. A payload mass of 750 kg has been found for the following target orbit: altitude $h = 1200$ km and inclination $i = 100$ deg. This three-stage case is different from the four-stage one, in particular for the value of the structural mass m_s to be left in orbit: 1107 kg for the three-stage and 349 kg for the four-stage launcher, and the final mass $m_f = m_s + m_u$ inserted in orbit is about 20% bigger in the three stage case. Despite this difference, the payload mass error for the three-stage example is 4%, that is, almost the same value of the four-stage case shown in Table 4.

V. Conclusions

Launcher performance evaluation can be achieved by trajectory optimization algorithms that are demanding in computational time and also require a specialist to choose suitable inputs to allow convergence of the optimization process. If a fast estimate of the performance of a launcher is required, allowing reasonable error, as may happen in the preliminary design of a launch vehicle, it is preferable to avoid long computations and to use a fast tool. The usual method of velocity loss balance results in excessive errors; to improve the launcher performance estimate, an algorithm has been introduced, based on the Culler–Fried[3] formula for the gravity turn trajectory. The Culler–Fried method has been generalized here to take into account multistaging and the possibility to use tabulated experimental data of thrust and mass variation. After the gravity turn, the trajectory is completed by a coasting and a guided phase (linear tangent steering law) so that the algorithm drives the launcher to the target orbit. Thus, in few seconds the following output is obtained: payload mass, azimuth angle, coasting time, and ΔV losses evaluation. Some tests have been run, and all of them show that the accuracy of the present method is well within 10% of relative error. The goal of an algorithm, which is fast and sufficiently accurate, seems to be achieved. Moreover, the output of the algorithm can be a good input for more complex and accurate trajectory optimization programs.

Appendix: Launcher Parameters

The four-stage launcher considered has the following relevant parameters:

1) The propellant masses of stages 1, 2, 3, and 4 are 87,036, 15,965, 7443, and 370 kg.

2) The structural masses of stages 1, 2, 3, and 4 are 13,556, 2058, 913, and 349 kg.

3) The heat shield mass is 440 kg.

4) The reference surfaces of stages 1 and 2 are 7.28 and 7.28 m^2.

5) The nozzle surfaces of stages 1 and 2 are 3.95 and 1.47 m^2.

6) The drag coefficients are as follows: at Mach 0.5 $C_D = 0.22$,

at Mach 1 $C_D = 0.64$, at Mach 2 $C_D = 0.52$, and at Mach 6 $C_D = 0.25$.

The three-stage launcher considered has the following relevant parameters.

1) The propellant masses of stages 1, 2, and 3 are 65,059, 23,000, and 6255 kg.

2) The structural masses of stages 1, 2, and 3 are 7309, 2874, and 1107 kg.

3) The heat shield mass is 385 kg.

4) The reference surfaces of stages 1 and 2 are 4.87 and 4.87 m^2.

5) The nozzle surfaces of stages 1–2: 2.15–1.72 m^2.

6) The drag coefficients are as follows: at Mach 0.5 $C_D = 0.26$, at Mach 1 $C_D = 0.89$, at Mach 2 $C_D = 0.67$, and at Mach 6 $C_D = 0.36$.

7) The first-stage average thrust value is 1,779,313 N.

8) The second-stage average thrust value is 924,765 N.

9) The third-stage average thrust value is 55,400 N.

Acknowledgments

The authors gratefully acknowledge C. Circi, F. Graziani, and A. Rinalducci for their comments.

References

[1]Bertotti, B., and Farinella, P., *Physics of the Earth and Solar System*, Kluwer, Dordrecht, The Netherlands, 1990, pp. 402–406.

[2]Cornelisse, J., Schoyer, H., and Wakker, K., *Rocket Propulsion and Spacecraft Dynamics*, Pitman, London, 1979, pp. 265–280, 389–405.

[3]Culler, G., and Fried, B., "Universal Gravity Turn Trajectories," *Journal of Applied Physics*, Vol. 18, No. 6, 1957, pp. 672–676.

[4]Thomson, W., *Introduction to Spaceflight Dynamics*, Wiley, New York, 1962, pp. 257–260.

[5]De Pasquale, E., "Launch Trajectories and Guidance Algorithms for Small Launchers," Ph.D. Dissertation, Scuola di Ingegneria Aerospaziale di Roma, University of Rome "La Sapienza," Rome, June 1998 (in Italian).

[6]Dorrington, G., "Optimal Thrust to Weight Ratio for Gravity Turn Trajectories," *Journal of Spacecraft and Rockets*, Vol. 37, No. 4, 2000, pp. 543, 544.

[7]Noton, M., *Spacecraft Navigation and Guidance*, Springer-Verlag, London, 1998, pp. 42–44.

[8]Rinalducci, A., "A Guidance System for Multistage Launchers," Laurea Dissertation, Scuola di Ingegneria Aerospaziale, University of Rome "La Sapienza," Rome, Feb. 1997 (in Italian).

[9]Teofilatto, P., and De Pasquale, E., "A Fast Guidance Algorithm for an Autonomous Navigation System," *Planetary and Space Science*, Vol. 46, No. 11, 1998, pp. 1627–1632.